HYBRID MODIFIED ELMAN NN CONTROLLER DESIGN ON PERMANENT MAGNET SYNCHRONOUS MOTOR DRIVEN ELECTRIC SCOOTER

Chih-Hong Lin[1] and Chih-Peng Lin[2]
[1]*Department of Electrical Engineering, National United University, Miaoli 360, Taiwan*
[2]*Department of Engineering, Su-Mo Enterprise Co. LTD, Taichung 430, Taiwan*
E-mail: jhlin@nuu.edu.tw; d8802801@yahoo.com.tw

Received November 2012, Accepted April 2013
No. 12-CSME-108, E.I.C. Accession Number 3428

ABSTRACT
The electric scooter driven by permanent magnet synchronous motor (PMSM) has nonlinear and time-varying characteristic. An accurate dynamic model is not easy to establish for electric scooter in the linear controller design. In order to conquer the above problem, a novel hybrid modified Elman neural network (NN) control scheme is proposed to control for electric scooter driven by PMSM. The proposed control system consists of a supervisor control, a modified Elman NN and a compensated control with adaptive law. Finally, the effectiveness of the proposed novel hybrid modified Elman NN control system is demonstrated in comparison with the PI controller from some experimental results.

Keywords: permanent magnet synchronous motor; modified Elman neural network; electric scooter.

CONCEPTION D'UN SYSTÈME DE COMMANDE ELMAN NN POUR MOTEUR SYNCHRONE À AIMANT PERMANENT POUR SCOOTER ÉLECTRIQUE

RÉSUMÉ
Un scooter électrique à moteur synchrone à aimant permanent possède des caractéristiques non-linéaires et variables dans le temps. Dans la conception d'un système de commande linéaire, un modèle dynamique précis n'est pas facile à réaliser. Dans le but de surmonter le problème, un schème de contrôle à réseau neuronal Elman modifié, est proposé pour scooter électrique à moteur PMSM. Le système de commande proposé consiste en un superviseur de commande, un Elman NN modifié et une commande compensée. Finalement, l'efficacité de ce système de commande hybride Elman NN a été démontrée en le comparant au système de commande PI par des résultats expérimentaux.

Mots-clés : moteur synchrone à aimant permanent ; réseau neuronal Elman modifié ; scooter électrique.

NOMENCLATURE

v_{d1}, v_{q1}	d- and q-axis stator voltages (V)
i_{d1}, i_{q1}	d- and q-axis stator currents (V)
L_{d1}, L_{q1}	d- and q-axis stator inductances (H)
R_1	stator resistance (Ω)
T_m	electromagnet torque (Nm)
P_1	number of poles
T_{L1}	external torque (Nm)
B_1	total viscous frictional coefficient (Nm/rad/sec)
J_1	total moment of inertia (Nm/rad/sec^2)
K_e	electrical constant (Nm/A)
i_{q1}^*	stator command current (A)
u_H	stator command current (A)
a_H, b_H, c_H	known mechanical constants
$f_1^U(\omega_1)$	known function
f_2^U, f_3	known constants
$e_1, \Delta e_1$	tracking error, tracking error change
u_H^*	ideal control law
$k_a, \bar{v}_{1a}$	positive constants
u_{1S}	supervisor control law
u_{2M}	modified Elman NN control law
u_{3C}	compensated control law
v_{1a}, v_{2a}	Lyapunov functions
d_{1S}	operating indicator
c_i^1, c_j^4	inputs of the modified Elman NN
$nod_i^1, nod_j^2,$ nod_k^3, nod_o^4	neurons of the modified Elman NN
$g_i^1, g_j^2, g_k^3, g_o^4$	activation functions of the modified Elman NN
$d_i^1, d_j^2, d_k^3, d_o^4$	outputs of the modified Elman NN
P_j, Q_j, R_j	differentiate the outputs with respect to the weights of the modified Elman NN
Greek symbols	
θ_f	rotor electrical position (rad)
θ^*	desired rotor mechanical position (rad)
θ_1	rotor mechanical position (rad)
λ_{fd1}	permanent magnet flux linkage (Wb)
ω_1^*	command rotor mechanical speed (rad/sec)
ω^*	desired rotor mechanical speed (rad/sec)
ω_1	rotor mechanical speed (rad/sec)
$\mu_{oi}, \mu_{ij}, \mu_{kj}, \mu_{jo}$	connective weights of the modified Elman NN
η	self-connecting feedback gain
α	positive constant
β	adaptation gain
σ	minimum approximation error
ψ	adjustable weight parameters vector
ψ^*	ideal weight vector
χ	input vector
$\dot{\psi}$	adaptive law (updated law)
$\Omega_1(t)$	function

1. INTRODUCTION

For the purpose of reducing petroleum dependence and air pollution, there are many countries to develop electric vehicles substitution of petroleum-power supply. Because the scooters are much more extensive than cars for personal transportation in Taiwan, I put my study on the development and research of electric scooter. Because of wheels of the electric scooters are driven by AC motor, the selections of AC motor drive system are very important jobs. The AC servo motors have been widely used in many applications of mechatronics, e.g. robotics, elevators and CNC, etc. [1, 2]. The permanent magnet synchronous motors (PMSMs) provide higher efficiency, higher power density and lower power loss for their size compared to switched reluctance motors (SRMs) and induction motors (IMs). Field-oriented control is the most popular control technique used with PMSMs. As a result, torque ripple can be extremely low, on par with that of SRMs and IMs. On the other hand, PMSMs controlled by field-oriented control, which can be achieved fast four-quadrant operation, are much less sensitive to the parameter variations of the motor [1–3].

The Elman neural network (NN) is a partial recurrent network model that was first proposed by Elman [4]. Typical Elman NN has one hidden layer with delayed feedback. The Elman NN is capable of providing the standard state-space representation for dynamic systems. The Elman NN can be considered to be a special type of recurrent neural network with feedback connections from the hidden layer to the context layer. The context layer is an additional layer that is used as an extra memory to memorize previous activations of the hidden neurons and feed to all the hidden neurons after the one-step time delay. Therefore, compared with the general recurrent neural networks [5–7], the Elman NN has a special explicit memory to store the temporal information. Due to the context neurons, it has certain dynamical advantages over static neural network [5–7] and it also has been widely applied in dynamical systems identification and control [8–10]. Generally, Elman NN can be considered to be a special kind of feed-forward neural network with additional memory neurons [4]. Furthermore, the Elman NN can approximate high-order systems with higher precision and faster speed of convergence.

The recurrent neural network has received increasing attention due to its structural advantage in nonlinear system modeling and dynamic system control [11–15]. The most important characteristic of the recurrent neural network is its self-connection to memorize feedback information of the historical influence in the same neuron. Moreover, in the general recurrent neural networks, the specific self-connection feedback of the hidden neuron or output neuron is responsible for memorizing the specific previous activation of the hidden neuron or output neuron and feed to itself only. Therefore, the outputs of the other neurons have no ability to affect the specific neuron. However, in the complicated nonlinear dynamic system such as PMSM driven electric scooter system, the flux linkage and external force interference are always a factor. Hence, if each neuron in the recurrent neural networks is considered as a state in the nonlinear dynamic systems, the self-connection feedback type is unable to approximate the dynamic systems efficiently. On the other hand, the feedbacks in Elman NN not only are self-connecting but they also store in the context neurons and feed to all the hidden neurons. Thus, the structure of Elman NN is more powerful than the general recurrent neural networks for dealing with time-varying, and nonlinear dynamic systems can be approximated efficiently with the additional context layer. In order to improve the ability of identifying high order systems, some modified Elman NNs [16–19] have been proposed recently, which proved to have more advantages than the basic Elman NN, including a better performance, higher accuracy, dynamic robustness, and a fast transient performance.

Due to real plants with many nonlinear dynamics, e.g. electric scooter [20, 21], the hybrid recurrent fuzzy neural network (RFNN) controller may not provide satisfactory control performance when operated over a wide range of operating conditions. In [20], the hybrid RFNN controller using rotor flux estimator control the PMSM without shaft encoder to drive electric scooter. In [21] the hybrid RFNN control is feedback control for PMSM driven electric scooter with shaft encoder. The favorable speed tracking responses can

be only achieved by using the hybrid RFNN controller in 1200 rpm at the nominal case and the parameter variation case, but poor speed tracking responses in 2400 rpm due to uncertainty perturbation. On the other hand, if the controlled plant has highly nonlinear uncertainties, the linear controller may also not provide satisfactory control performance. Therefore, to ensure the control performance of robustness, the PMSM controlled by Elman NN control system is developed to drive electric scooter in this paper. A novel hybrid modified Elman NN control system has fast learning property and good generalization capability. The control method, which is not dependent upon the predetermined characteristics of the motor, can adapt to any change in the motor characteristics. A novel hybrid modified Elman NN control system, which is composed of a supervised control system, a modified Elman NN controller, and a compensated controller with adaptive law, is applied to the PMSM drive electric scooter system. The on-line parameter training methodology of the modified Elman NN can be derived by using adaptation law according to the Lyapunov stability theorem and the gradient descent method. The modified Elman NN has the on-line learning ability to respond to the system's nonlinear and time-varying behaviors according to different speeds in electric scooter. Finally, performance of the proposed novel hybrid modified Elman NN control system is verified by experimental results.

2. CONFIGURATION OF FIELD-ORIENTED PMSM DRIVE SYSTEM

The voltage equations of a PMSM can be described in the rotor rotating reference frame as follows [1–3, 20, 21]:

$$v_{q1} = R_1 i_{q1} + L_{q1}\dot{i}_{q1} + \omega_1(L_{d1} i_{d1} + \lambda_{fd1}), \tag{1}$$

$$v_{d1} = R_1 i_{d1} + L_{d1}\dot{i}_{d1} - \omega_1 L_{q1} i_{q1}, \tag{2}$$

where v_{d1} and v_{q1} are the d- and q-axis stator voltages, i_{d1} and i_{q1} are the d- and q-axis stator currents, L_{d1} and L_{q1} are the d- and q-axis stator inductances, λ_{fd1} is the permanent magnet flux linkage, R_1 is the stator resistance, ω_1 is the rotor mechanical speed. The electromagnet torque T_m of a PMSM can be described as

$$T_m = \frac{3}{2}\frac{P_1}{2}[\lambda_{fd1}\, i_{q1} + (L_{d1} - L_{q1}) i_{d1}\, i_{q1}]. \tag{3}$$

The equation of the motor dynamics is

$$T_m = T_{L1} - B_l \omega_1 + J_1 \dot{\omega}_1 \tag{4}$$

where P_1 is the number of poles, T_{L1} is the external load disturbance, e.g. electric scooter, B_1 represents the total viscous frictional coefficient and J_1 is the total moment of inertia. The control principle of the PM synchronous motor drive system is based on field orientation. Due to $L_{d1} = L_{q1}$ and $I_{d1} = 0$ in surface-mounted type PMSM, the second term of Eq. (3) is zero. Therefore, the electromagnetic torque T_m is linearly proportional to q-axis current i_{q1}. When the d-axis rotor flux is constant, the maximum torque per ampere can be reached for the field-oriented control [3]. Then Eq. (3) can be simplified as

$$T_m = K_e\, i^*_{q1}, \tag{5}$$

$$K_e = 3P_1\lambda_{fd1}/4, \tag{6}$$

where K_e is the electrical constant. The block diagram of a PMSM driven electric scooter system is described in Fig. 1. The whole system of a PMSM driven electric scooter can be indicated as follows: a field-oriented institution, a PID current-loop control, a sine PWM control circuit, the interlock and isolated circuit, an IGBT power module inverter and a speed control loop [20, 21]. The PID current-loop controller is the current loop tracking controller. The field-oriented institution consists of the coordinate transformation, $\sin(\theta_f)/\cos(\theta_f)$ generation and lookup table generation. The field-oriented institution control and speed control are implemented by using TMS320C32 DSP control system. The PMSM driven electric scooter manipulated at load disturbance torque with nonlinear uncertainties.

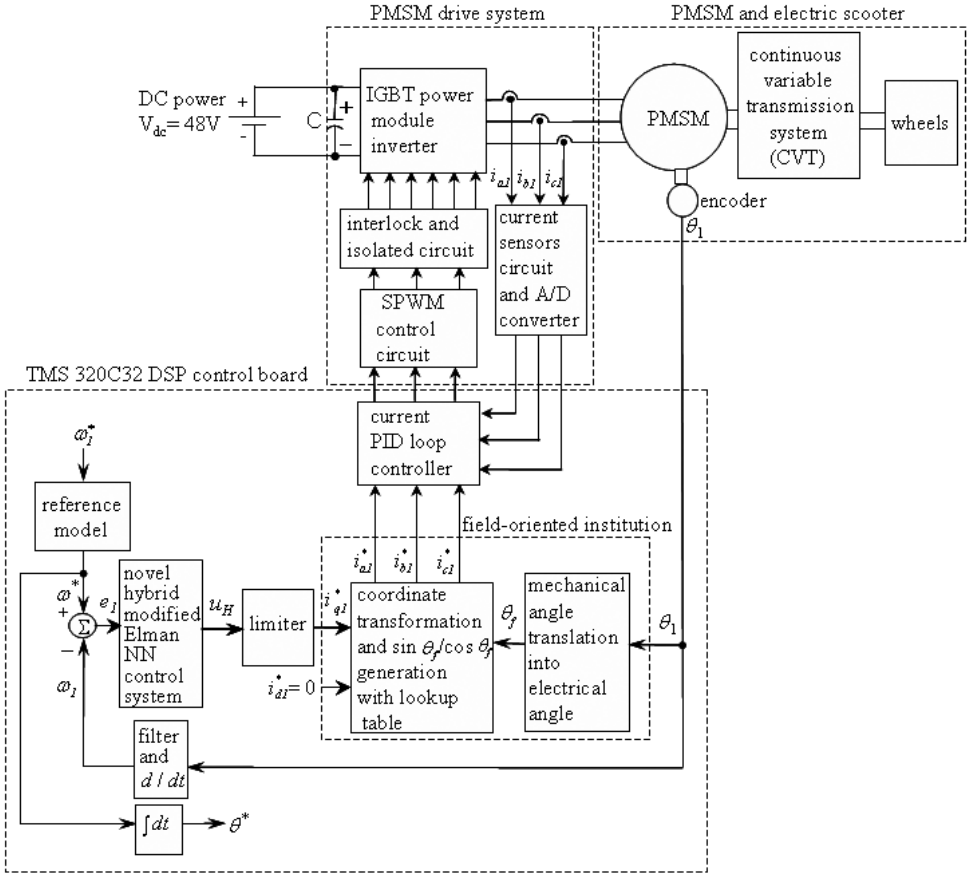

Fig. 1. Block diagram of a PMSM drive electric scooter system.

3. A NOVEL HYBRID MODIFIED ELMAN NN CONTROL SYSTEM DESIGN

For convenient design and analysis, the dynamic equation of the PMSM drive electric scooter system shown in Eq. (2) can be rewritten as

$$\dot{\omega}_1 = -B_1\omega_1/J_1 + K_e i_{q1}^*/J_1 - T_{L1}/J_1 = a_H\omega_1 + b_H u_H + c_H T_{L1}. \tag{7}$$

The $u_H = i_{q1}^*$ is the command current of the stator of the PMSM. The $a_H = -B_1/J_1$, $b_H = K_e/J_1$ and $c_H = -1/J_1$ are known constants and the parameters are assumed to be bounded in the uncertainties occurrence, i.e. $|a_H\omega_1| \le f_1^U(\omega_1), |c_H T_{L1}| \le f_2^U, f_3 \le b_H$, where $f_1^U(\omega_1)$ is a known continuous function, f_2^U and f_3 are known constants. Then, the tracking error can be defined as follows:

$$e_1 = \omega^* - \omega_1, \tag{8}$$

where ω^* represents the desired rotor speed; e_1 is the tracking error between the desired rotor speed and rotor speed. If the all parameters of the PMSM driven system includes external load disturbance are well known, the ideal control law can be designed as [20, 21]

$$u_H^* = [-a_H\omega_1 - c_H T_{L1} + \dot{\omega}^* + k_a e_1]/b_H \tag{9}$$

in which k_a is a positive constant. Replacing Eq. (9) by Eq. (7), the error dynamic equation can be obtained

$$\dot{e}_1 + k_a e_1 = 0. \tag{10}$$

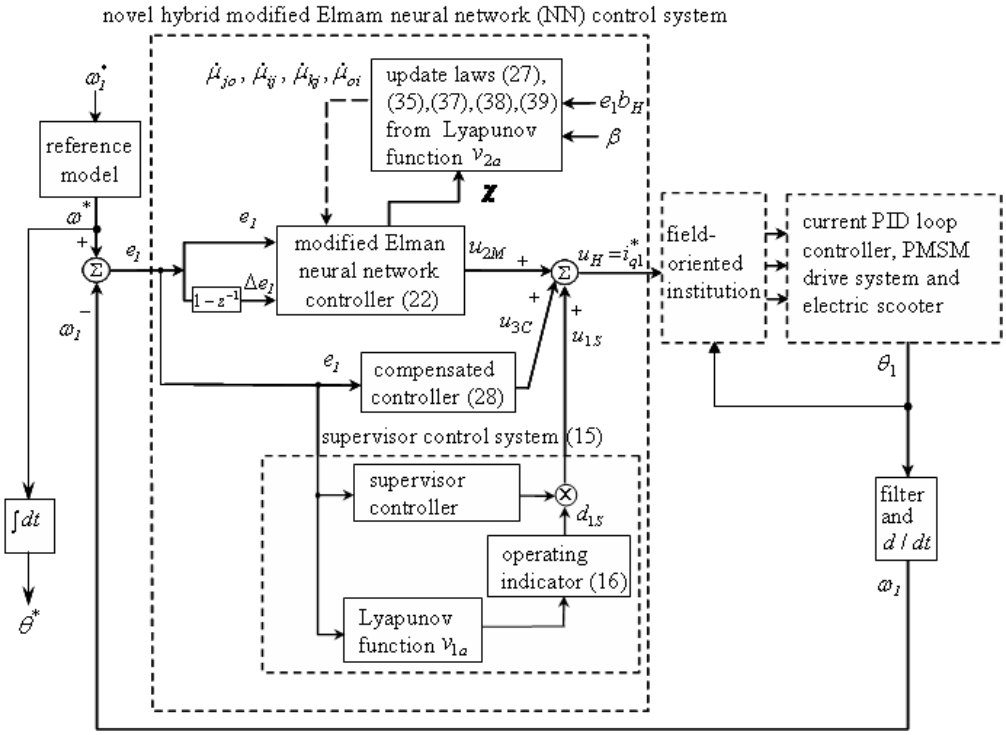

Fig. 2. Block diagram of novel hybrid modified Elman NN control system.

The system state can track the desired trajectory gradually if $e_1(t) \to 0$ as $t \to \infty$. However, the novel hybrid modified Elman NN control system is proposed to control PMSM driven electric scooter with nonlinear uncertainty. The configuration of the proposed novel hybrid modified Elman NN control system is described in Fig. 2.

The novel hybrid modified Elman NN control system composed of a modified Elman NN controller, a compensated controller and a supervisor control system. The control law is designed as follows [20–22]:

$$u_H = u_{1S} + u_{2M} + u_{3C}. \tag{11}$$

The designed idea of the proposed supervisor control u_{1S} is that capable to stabilize around a predetermined bound area in the states of the controlled system. Since supervised control caused the overdone and chattering control effort, the modified Elman NN control and compensated control are proposed to reduce and smooth the control effort when the system states are inside the predetermined bound area. The modified Elman NN control u_{2M} is the major tracking controller. It is used to imitate an ideal control law. The compensated control u_{3C} is designed to compensate the difference between the ideal control law and the modified Elman NN control. When the modified Elman NN approximation properties can not be ensured, the supervised control law is able to action in this case.

For the condition of divergence of states, the design of a novel hybrid modified Elman NN control system is essential to stretch the divergent states back to the predestinated bound area. The novel hybrid modified Elman NN control system can uniformly approximate the ideal control law inside the bound area. Then stability of the novel hybrid modified Elman NN control system can be warranted. An error dynamic equation can be acquired from Eqs. (7–11) as

$$\dot{e}_1 = -k_a e_1 + [u_H^* - u_{1S} - u_{2M} - u_{3C}]b_H. \tag{12}$$

Then the Lyapunov function is chosen as

$$v_{1a} = e_1^2/2\,. \tag{13}$$

Differentiating Eq. (13) with respect to t and substituting Eq. (12) into Eq. (13), we then obtain

$$\begin{aligned} \dot{v}_{1a} &= e_1\dot{e}_1 = e_1[-k_a e_1 + [u_H^* - u_{2M} - u_{3C} - u_{1S}]b_H] \\ &\leq -k_a e_1^2 + |e_1 b_H| \cdot [|u_H^*| + |u_{2M} + u_{3C}|] - e_1 b_H u_{1S}. \end{aligned} \tag{14}$$

To satisfy $\dot{v}_{1a} \leq 0$, the supervised control u_{1S} is designed as follows [21, 22]:

$$u_{1S} = d_{1S}\,\mathrm{sgn}(e_1 b_H)[|u_{2M} + u_{3C}| + (f_1^U(\omega_1) + f_2^U + |\dot{\omega}^*| + |k_a e_1|)/b_H], \tag{15}$$

in which sgn $(\cdot)$ is a sign function, and the operating indicator can be adopted as

$$d_{1S} = \begin{cases} d_{1S} = 1, & \text{if } v_{1a} \geq \bar{v}_{1a} \\ d_{1S} = 0, & \text{if } v_{1a} < \bar{v}_{1a} \end{cases} \tag{16}$$

where $\bar{v}_{1a}$ is a positive constant. Selecting $d_{1S} = 1$ and using Eq. (15), Eq. (14) can be obtained as

$$\begin{aligned} \dot{v}_{1a} &\leq -k_a e_1^2 + |e_1 b_H|[|u_H^*| + |u_{2M} + u_{3C}|] - e_1 b_H u_{1S} \\ &\leq -k_a e_1^2 + |e_1 b_H|[|a_H \omega_1| + |c_H T_L| + |\dot{\omega}^*| + |k_a e_1|]/b_H + [|u_{2M} + u_{3C}|] - [|u_{2M} + u_{3C}|] \\ &\quad - |e_1 b_H|[f_1^U(\omega_1) + f_2^U + |\dot{\omega}^*| + |k_a e_1|]/b_H \\ &\leq -k_a e_1^2 \leq 0. \end{aligned} \tag{17}$$

The supervised control system is capable to cause the tracking error to zero according to Eq. (17) without using modified Elman NN control and compensated control system. Due to the selection of the bound values, e.g. $f_1^U(\omega_1), f_2^U, f_3$ and sign function, the supervised control can produce in overdone and chattering control effort. Therefore, the modified Elman NN controller and compensated controller can be devised to conquer the mentioned blemish. The modified Elman NN control raised to imitate the ideal control u_H^*. Then the compensated control posed to compensate the difference between the ideal control u_H^* and the modified Elman NN control. The architecture of the proposed four-layer modified Elman NN is depicted in Fig. 3. It is composed of an input, a hidden, a context and an output layer. The activation functions and signal actions of nodes in each layer of the modified Elman NN can be described as:

First layer: input layer.
Each node i in this layer is indicated by using Π, which multiplies by each other between each other for input signals. Then outputs signals are the results of product. The input and the output for each node i in this layer are expressed as

$$\begin{aligned} nod_i^1(N) &= \Pi c_i^1(N)\mu_{oi}\, d_o^4(N-1), \\ d_i^1(N) &= g_i^1(nod_i^1(N)) = nod_i^1(N), \quad i = 1,2. \end{aligned} \tag{18}$$

The $c_1^1 = \omega - \omega_1 = e_1$ is the tracking error between the desired speed ω and the rotor speed ω_1. The $c_2^1 = e_1(1 - z^{-1}) = \Delta e_1$ is the tracking error change. μ_{oi} is the recurrent weight between output layer and input layer. The N denotes the number of iterations. The d_o^4 is the output value from output layer of the modified Elman NN.

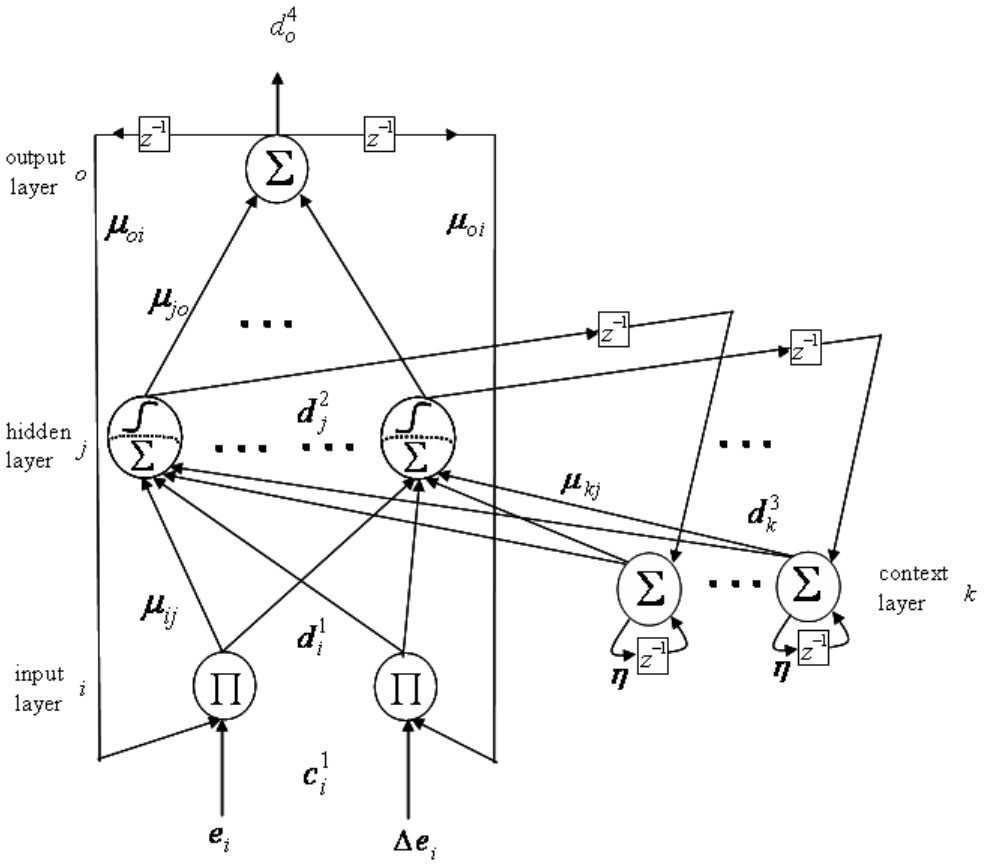

Fig. 3. Structure of the four-layer modified Elman NN.

Second layer: hidden layer.
The single node jth in this layer is labeled with $\sum$. It computes outputs of the input layer and the context layer as the summation of all input signals. The net input and the net output for node jth in this layer are expressed as

$$\begin{aligned} nod_j^2(N) &= \sum_k \mu_{kj} d_k^3(N) + \sum_i \mu_{ij} d_i^1(N), \\ d_j^2(N) &= g_j^2(nod_j^2(N)) = \frac{1}{1+e^{-nod_j^2(N)}}, \quad j = 1,2,\ldots,m\,, \end{aligned} \tag{19}$$

where μ_{kj} are the connective weights between the context layer and the hidden layer; μ_{ij} are the connective weights between the input layer and the hidden layer; m is the number of neurons in the hidden layer; g_j^2 is the activation function, which is also a sigmoid function; $d_i^1(N) = c_i^2(N)$ represents the ith output node of input layer; $d_k^3(N) = c_k^3(N)$ represents the kth input to the node of context layer.

Third layer: context layer.
In the context layer, the node input and the node output are represented as

$$\begin{aligned} nod_k^3(N) &= d_j^2(N-1) + \eta d_k^3(N-1) \\ d_k^3(N) &= g_k^3(nod_k^3(N)) = nod_k^3(N), \quad k = 1,\ldots,n, \end{aligned} \tag{20}$$

where $d_j^2(N) = c_j^4(N)$ represents the jth output node of hidden layer; $d_k^3(N)$ represents the kth output to the node of context layer. n is the number of neurons in the context layer; where $0 \leq \eta < 1$ is the self-connecting feedback gain of context layer.

Fourth layer: output layer.
The single node oth in this layer is labeled with $\sum$. It computes the overall output as the summation of all input signals. The net input and the net output for node oth in this layer are expressed as

$$nod_o^4(N) = \sum_j \mu_{jo} c_j^4(N),$$
$$d_o^4(N) = g_o^4(nod_o^4(N)) = nod_o^4, \quad o = 1, \tag{21}$$

where μ_{jo} are the connective weights between the hidden layer and the output layer; g_o^4 is the activation function, which is set to be unit; $d_j^2(N) = c_j^4(N)$ represents the jth input to the node of output layer. The output value of the modified Elman NN can be represented as $d_o^4 = u_{2M}$. Then the output value of the modified Elman NN, u_{2M}, can be denoted as

$$u_{2M} = (\psi)^T \chi. \tag{22}$$

The $\psi = [\mu_{11}^4 \quad \mu_{21}^4 \quad \cdots \quad \mu_{m1}^4]^T$ is the adjustable weight parameters vector between the hidden layer and the output layer of the modified Elman NN. The $\chi = [c_1^4 c_2^4 \cdots c_m^4]^T$ is the inputs vector in the output layer of the modified Elman NN, in which c_j^4 is determined by the selected sigmoid function and $0 \leq c_j^4 \leq 1$.

In order to evolve the compensated control u_{3C}, a minimum approximation error σ is defined as

$$\sigma = u_H^* - u_{2M}^* = u_H^* - (\psi^*)^T \chi \ . \tag{23}$$

The ψ^* is an ideal weight vector to reach of minimum approximation error. We assumed that the absolute value σ is less than a positive constant α, i.e., $|\sigma| < \alpha$. Then, the error dynamic equation can be rewritten as

$$\begin{aligned}
\dot{e}_1 &= -k_a e_1 + b_H\{[u_H^* - u_{2M}] - u_{3C} - u_{1S}\} \\
&= -k_a e_1 + b_H\{[u_H^* - u_{2M}^* + u_{2M}^* - u_{2M}] - u_{3C} - u_{1S}\} \\
&= -k_a e_1 + b_H\{[u_H^* - u_{2M}^* + (\psi^*)^T \chi - (\psi)^T \chi] - u_{3C} - u_{1S}\} \\
&= -k_a e_1 + b_H\{\sigma + (\psi^* - \psi)^T \chi - u_{3C} - u_{1S}\} \ .
\end{aligned} \tag{24}$$

Then, the Lyapunov function is selected as

$$v_{2a} = e_1^2/2 + (\psi^* - \psi)^T (\psi^* - \psi)/(2\beta). \tag{25}$$

Differentiating the Lyapunov function with respect to t and using Eq. (24), Eq. (25) can then be rewritten as

$$\begin{aligned}
\dot{v}_{2a} &= e_1 \dot{e}_1 - (\psi^* - \psi)^T \dot{\psi}/\beta \\
&= -k_a e_1^2 + e_1 b_H\{\sigma - u_{3C} - u_{1S}\} + e_1 b_H (\psi^* - \psi)^T \chi - (\psi^* - \psi)^T \dot{\psi}/\beta.
\end{aligned} \tag{26}$$

The updated law $\dot{\psi}$ and the compensated controller u_{3C} to satisfy $\dot{v}_{2a} \leq 0$ can be designed as

$$\dot{\psi} = \beta e_1 b_H \chi, \tag{27}$$

$$u_{3C} = \alpha \ \mathrm{sgn}(e_1 b_H) \tag{28}$$

in which $\beta > 0$ is denoted as adaptation gain. Using Eqs. (15) and Eq. (27), Eq. (26) can be represented as

$$\dot{v}_{2a} = -k_a e_1^2 + e_1 b_H \{\sigma - u_{3C} - u_{1S}\} \leq -k_a e_1^2 + e_1 b_H \{\sigma - u_{3C}\}. \tag{29}$$

From Eqn. (28), the Eqn. (29) can be obtained as

$$\dot{v}_{2a} \leq -k_a e_1^2 + e_1 b_H \{\sigma - u_{3C}\} \leq -k_a e_1^2 + |e_1 b_H| \{|\sigma| - \alpha\} \leq -k_a e_1^2 \leq 0 \ . \tag{30}$$

From Eq. (30), the $\dot{v}_{2a}$ is negative semi-definite, i.e. $v_{2a}(t) \leq v_{2a}(0)$. It implies that e_1 and $(\psi^* - \psi)$ be bounded. For proof the novel hybrid modified Elman NN control system to be gradually stable, let function is defined as

$$\Omega_1(t) = -\dot{v}_{2a}(t) = k_a e_1^2 \tag{31}$$

Integrating Eq. (31) with respect to t gives

$$\int_0^t \Omega_1(t) dt = \int_0^t -\dot{v}_{2a}(t) dt = v_{2a}(0) - v_{2a}(t) \tag{32}$$

Due to $v_{2a}(0)$ is bounded, and $v_{2a}(t)$ is nonincreasing and bounded, then

$$\lim_{t \to \infty} \int_0^t \Omega_1(t) dt < \infty \tag{33}$$

Differentiating Eq. (31) with respect to t gives

$$\dot{\Omega}_1(t) = 2 k_a e_1 \dot{e}_1 \ . \tag{34}$$

Due to all the variables in the right side of Eq. (24) are bounded. It implies that $\dot{e}_1$ is also bounded. Then, $\Omega_1(t)$ is a uniformly continuous function [23, 24]. It is denoted that $\lim_{t \to \infty} \Omega_1(t) = 0$ by using Barbalat's lemma [23, 24]. Therefore $e_1(t) \to 0$ as $t \to \infty$. From above proof, the novel hybrid modified Elman NN control system is gradually stable. Moreover, the tracking error e_1 of the system will converge to zero according to $e_1(t) = 0$.

According to Lyapunov stability theorem and the gradient descent method, an on-line parameter training methodology of the modified Elman NN can be derived and trained effectively. Then the updated laws of the parameters $\dot{\psi}(\mu_{jo}, \mu_{kj}, \mu_{ij}, \mu_{oi})$ can be computed by using the gradient descent method and the back-propagation algorithm as follows

$$\dot{\mu}_{jo} = \beta e_1 b_H \chi \triangleq -\beta \frac{\partial v_{2a}}{\partial u_{2M}} \frac{\partial u_{2M}}{\partial d_o^4} \frac{\partial d_o^4}{\partial nod_0^4} \frac{\partial nod_o^4}{\partial \mu_{jo}} = -\beta \frac{\partial v_{2a}}{\partial u_{2M}} c_k^4 \ . \tag{35}$$

The above Jacobian term of control system can be rewritten as $\partial v_{2a} / \partial u_{2M} = -e_1 b_H$. Then, the first error term can be counted as

$$\upsilon_k \triangleq -\frac{\partial v_{2a}}{\partial u_{2M}} \frac{\partial u_{2M}}{\partial d_o^4} \frac{\partial d_o^4}{\partial nod_o^4} \frac{\partial nod_o^4}{\partial d_k^3} \frac{\partial d_k^3}{\partial nod_k^3} = e_1 b_H \mu_{jo} \ . \tag{36}$$

The connective weight μ_{kj} between context layer and hidden layer can be updated as

$$\dot{\mu}_{kj} = -\frac{\partial v_{2a}}{\partial \mu_{kj}} = -\frac{\partial v_{2a}}{\partial u_{2M}} \frac{\partial u_{2M}}{\partial d_o^4} \frac{\partial g_o^4}{\partial nod_o^4} \frac{\partial nod_o^4}{\partial d_j^2} \frac{\partial d_j^2}{\partial nod_j^2} \frac{\partial nod_j^2}{\partial \mu_{kj}} = \beta \mu_{jo} P_j, \tag{37}$$

where $P_j \equiv \partial d_j^2 / \partial \mu_{kj}$; this can be calculated from Eq. (19).

The connective weight μ_{ij} between hidden layer and input layer can be updated as

$$\dot{\mu}_{ij} = -\frac{\partial \nu_{2a}}{\partial \mu_{ij}} = -\frac{\partial \nu_{2a}}{\partial u_{2M}} \frac{\partial u_{2M}}{\partial d_o^4} \frac{\partial d_o^4}{\partial nod_o^4} \frac{\partial nod_o^4}{\partial d_j^2} \frac{\partial d_j^2}{\partial nod_j^2} \frac{\partial nod_j^2}{\partial \mu_{ij}} = \beta \mu_{jo} Q_j, \tag{38}$$

where $Q_j \equiv \partial d_j^2 / \mu_{ij}$, it can be calculated from Eq. (19).

The recurrent weight μ_{oi} between output layer and input layer can be updated as

$$\dot{\mu}_{oi} = -\frac{\partial \nu_{2a}}{\partial \mu_{oi}} = -\frac{\partial \nu_{2a}}{\partial u_{2M}} \frac{\partial u_{2M}}{\partial d_o^4} \frac{\partial d_o^4}{\partial d_j^2} \frac{\partial d_j^2}{\partial d_i^1} \frac{\partial d_i^1}{\partial \mu_{oi}} = \beta \mu_{jo} R_j, \tag{39}$$

where $R_j \equiv \partial d_j^2 / \mu_{oi}$; this can be calculated from Eqs. (18) and (19).

4. EXPERIMENTAL RESULTS

The whole system of the DSP-based control system for a PMSM drive electric scooter system is shown in Fig. 1. The control algorithm was executed by a TMS320C32 DSP control system includes multi-channels of D/A, eight channels programmable PWM and encoder interface circuits. The IGBT power modules voltage source inverter is executed by current-controlled SPWM with a switching frequency of 15 kHz. The control gains of PID current-loop controller are $k_P = 15, k_I = 2, k_D = 0.5$ to attain good current dynamic response by using try and error method. The specification of PMSM is a three-phase two poles 48V 750W 16.5 A 3600 rpm. The parameters of the PMSM are $R_1 = 2.5\Omega$, $L_{d1} = L_{q1} = 6.53$ mH, $K_e = 0.86$ Nm/A, $\bar{J}_1 = 2.15 \times 10^{-3}$ Nmsec, $\bar{B}_1 = 6.18 \times 10^{-3}$ Nmsec/rad. Due to inherent uncertainty in electric scooter and output current limitation of battery power capacity, the PMSM can only operate at 251.2 rad/sec (2400 rpm).

To show the control performance of the proposed novel hybrid modified Elman NN control system, two cases are provided in the experimentation, which are the 125.6 rad/sec (1200 rpm) case and the 251.2 rad/sec (2400 rpm) case. Since the electric scooter is a nonlinear time varying system, the control gains of the PI and the PID controllers for the speed tracking are obtained by try and error in order to achieve good transient and steady-state control performance at the 125.6 rad/sec (1200 rpm) case. Firstly, the control gains of the PI controller are $k_{P1} = 12.5, k_{I1} = 1.2$ at the 125.6 rad/sec (1200 rpm) case for the speed tracking. The experimental results of the PI controller for a PMSM driven electric scooter at the 125.6 rad/sec (1200 rpm) case and the 251.2 rad/sec (2400 rpm) case are shown in Figs. 4 and 5, where tracking responses of the command rotor speed ω_1^*; the desired rotor speed ω^* and the measured rotor speed ω_1 shown in Figs. 4(a) and 5(a); tracking responses of the desired rotor position θ^* and the measured rotor position θ_1 shown in Figs. 4(b) and 5(b); tracking responses of the command current i_{a1}^* and the measured current i_{a1} in phase $a1$ shown in Figs. 4(c) and 5(c); tracking responses of the command current i_{b1}^* and measured current i_{b1} in phase b1 shown in Figs. 4(d) and 5(d), respectively.

Since the low speed operation is the same as the nominal case due to smaller disturbance, the speed and current responses shown in Figs. 4(a), 4(c) and 4(d) have better tracking performance. Moreover, the degenerate tracking responses shown in Figs. 5(a), 5(c) and 5(d) are obvious due to the occurrence of parameter variation and external load disturbance. From the experimental results, sluggish speed and current tracking responses are obtained for the PI controlled PMSM driven electric scooter due to the weak robustness of the linear controller.

The control gains of the proposed novel hybrid modified Elman NN control system are $\alpha = 0.1$, $\beta = 0.5$, $\sigma = 0.05$, $\eta = 0.1$. All control gains of the novel hybrid modified Elman NN control system are chosen to achieve the best transient control performance in experimentation considering the requirement of stability. The parameter adjustment process remains continually active for the duration of the experimentation. The

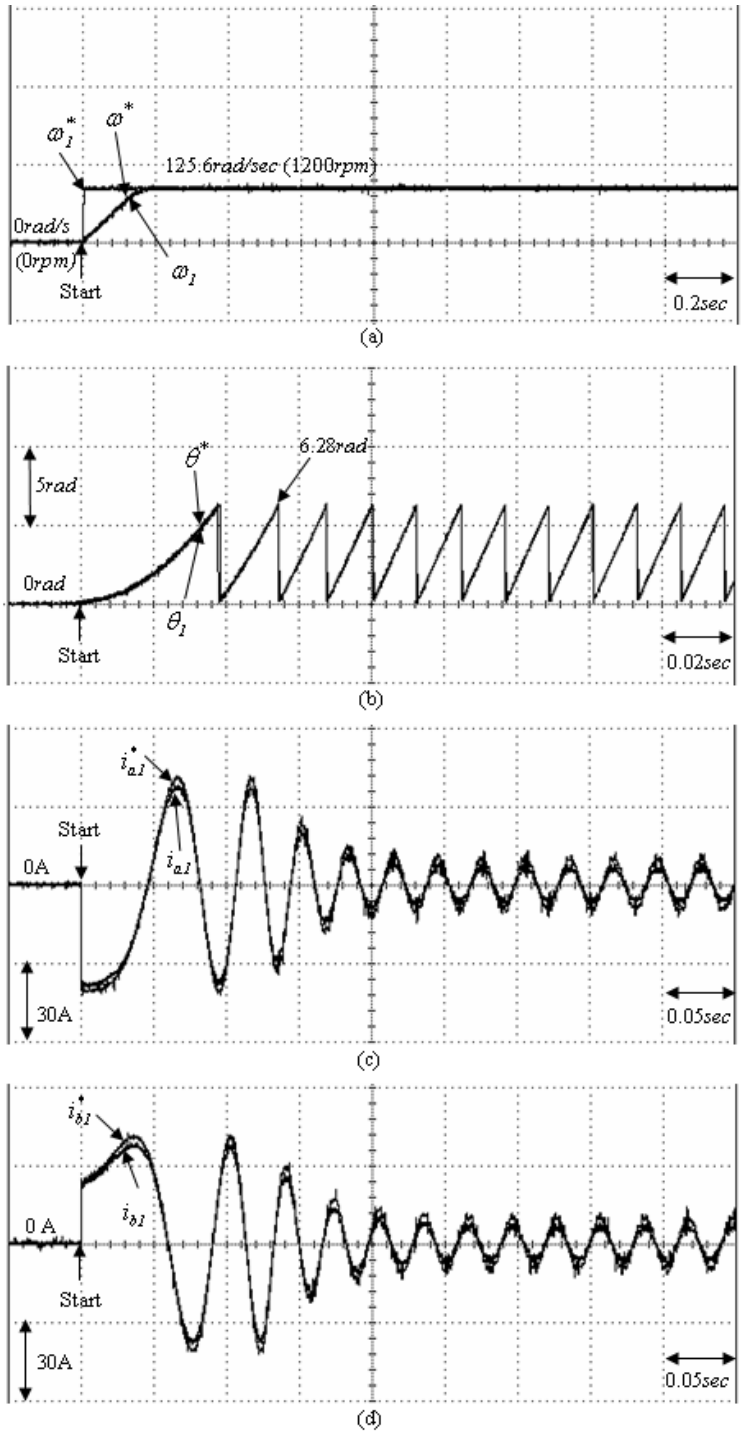

Fig. 4. Experimental results of the PI controlled for a PMSM drive electric scooter at 125.6 rad/sec (1200 rpm): (a) command rotor speed ω_1^*, desired rotor speed ω^* and measured rotor speed ω_1; (b) command rotor position θ^*, measured rotor position θ_1; (c) command current i_{a1}^* and measured current i_{a1} in phase $a1$; (d) command current i_{b1}^* and measured current i_{b1} in phase $b1$.

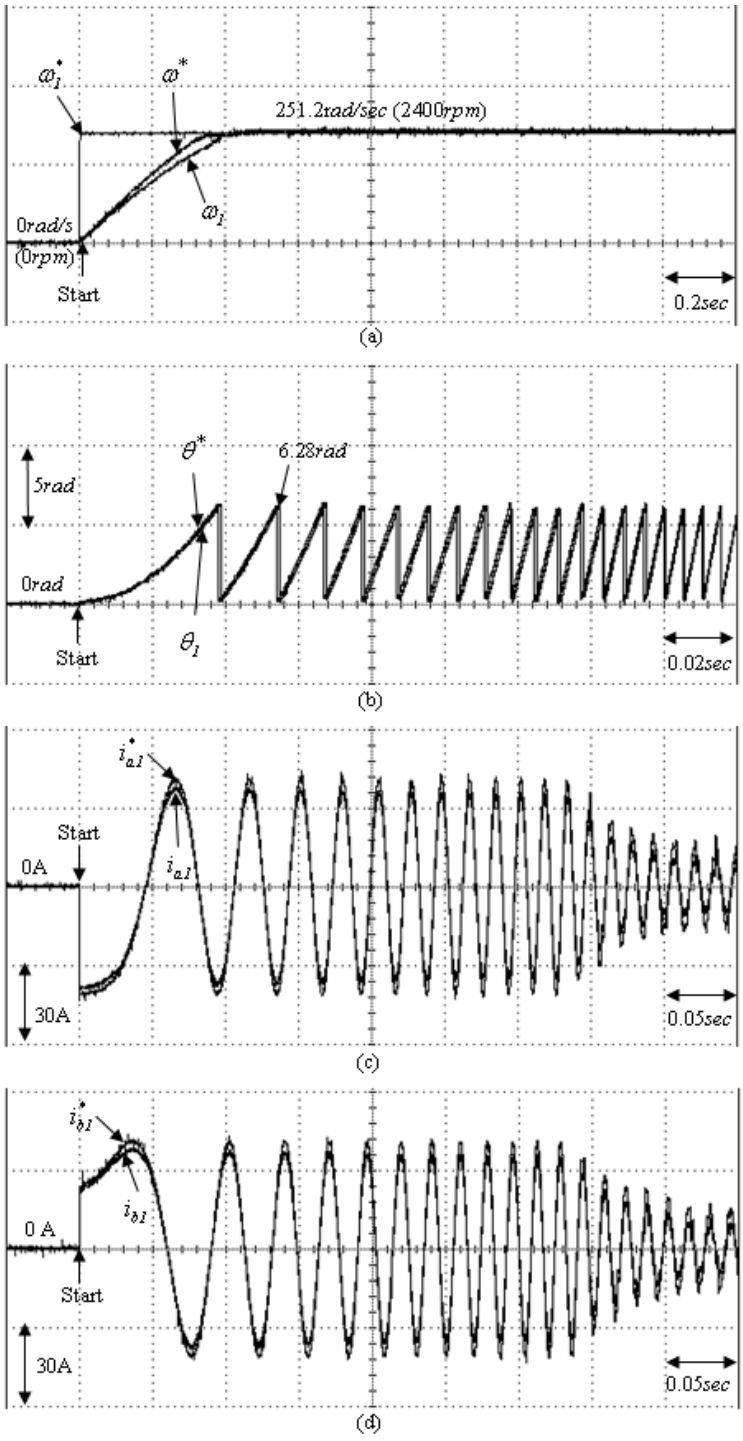

Fig. 5. Experimental results of the PI controlled for a PMSM drive electric scooter at 251.2 rad/sec (2400 rpm): (a) command rotor speed ω_1^*, desired rotor speed ω^* and measured rotor speed ω_1; (b) command rotor position θ^*, measured rotor position θ_1; (c) command current i_{a1}^* and measured current i_{a1} in phase $a1$; (d) command current i_{b1}^* and measured current i_{b1} in phase $b1$.

structure of modified Elman NN controller has 2 nodes, 7 nodes, 7 nodes and 1 node in the input layer, the hidden layer, the context layer and the output layer, respectively. The experimental results of the modified Elman NN in novel hybrid modified Elman NN control system for a PMSM driven electric scooter at the 125.6 rad/sec (1200 rpm) case and the 251.2 rad/sec (2400 rpm) case are shown in Figs. 6 and 7, where tracking responses of the command rotor speed ω_1^*, the desired rotor speed ω^* and the measured rotor speed ω_1 shown in Figs. 6(a) and 7(a); tracking responses of the desired rotor position θ^* and the measured rotor position θ_1 shown in Figs. 6(b) and 7(b); tracking responses of the command current i_{a1}^* and the measured current i_{a1} in phase $a1$ shown in Figs. 6(c) and 7(c); tracking responses of the command current i_{b1}^* and measured current i_{b1}^* in phase $b1$ shown in Figs. 6(d) and 7(d), respectively. The better speed and current tracking responses are shown in Figs. 6(a), 6(c), 6(d) and 7(a), 7(c), 7(d) in spite of the occurrence of parameter variation and external load disturbance. From the experimental results, the accurate tracking performance is obtained for the novel modified Elman NN controlled PMSM driven electric scooter owing to the on-line adaptive mechanism of modified Elman NN and action of the compensated controller. Therefore these results show that the novel hybrid modified Elman NN control system has better control performance than the PI controller to speed perturbation for a PMSM driven electric scooter. Additionally, the small chattering phenomena existed in phase $a1$ and in phase $b1$ as shown in Figs. 7(c) and 7(d) are induced by on-line adjusted of the modified Elman NN to cope with the high-frequency unmodelled dynamic of the controlled plant.

The measured rotor speeds and currents responses under step disturbance torque are given finally. Two test conditions are given as the $T_{L1} = 2$ Nm load torque disturbance, command rotor speed $\omega_1^* = 125.6$ rad/sec (1200 rpm) and $T_{L1} = 4$ Nm load torque disturbance, command rotor speed $\omega_1^* = 251.2$ rad/sec (2400 rpm) with adding load and shedding load. The experimental results under $T_{L1} = 2$ Nm and $T_{L1} = 4$ Nm load torque disturbances with adding load and shedding load at the command rotor speed $\omega_1^* = 125.6$ rad/sec (1200 rpm) and command rotor speed $\omega_L^* = 251.2$ rad/sec (2400 rpm) are shown in Fig. 8 by using the PI controller and the novel hybrid modified Elman NN control system. The measured rotor speed response and measured current in phase $a1$ for using the PI controller under $T_{L1} = 2$ Nm load torque disturbance with adding load and shedding load at the command rotor speed $\omega_1^* = 125.6$ rad/sec (1200 rpm) is shown in Fig. 8(a). The measured rotor speed response and measured current in phase $a1$ for using the proposed novel hybrid modified Elman NN control system under $T_{l1} = 2$ Nm load torque disturbance with adding load and shedding load at the command rotor speed $\omega_1^* = 125.6$ rad/sec (1200 rpm) is shown in Fig. 8(b). The measured rotor speed response and measured current in phase $a1$ for using the PI controller under $T_{L1} = 4$ Nm load torque disturbance with adding load and shedding load at the command rotor speed $\omega_1^* = 251.2$ rad/sec (2400 rpm) is shown in Fig. 8(c). The measured rotor speed response and measured current in phase $a1$ for using the proposed novel hybrid modified Elman NN control system under $T_{L1} = 4$ Nm load torque disturbance with adding load and shedding load at the command rotor speed $\omega_1^* = 251.2$ rad/sec (2400 rpm) is shown in Fig. 8(d). From the experimental results, the degenerated responses under $T_{L1} = 2$ Nm and $T_{L1} = 4$ Nm load torque disturbances at the command rotor speed $\omega_1^* = 125.6$ rad/sec (1200 rpm) and $\omega_1^* = 251.2$ rad/sec (2400 rpm) are obvious by using PI controller shown in Figs. 8(a) and 8(c). The control performance using the novel hybrid modified Elman NN control system are much improved responses under $T_{L1} = 2$ Nm and $T_{L1} = 4$ Nm load torque disturbances at the command rotor speed $\omega_1^* = 125.6$ rad/sec (1200 rpm) and $\omega_1^* = 251.2$ rad/sec (2400 rpm). Moreover, transient response of the novel hybrid modified Elman NN control system is better control performance than PI control system under $T_{L1} = 2$ Nm and $T_{L1} = 4$ Nm load torque disturbances at the command rotor speed $\omega_1^* = 125.6$ rad/sec (1200 rpm) and $\omega_1^* = 251.2$ rad/sec (2400 rpm).

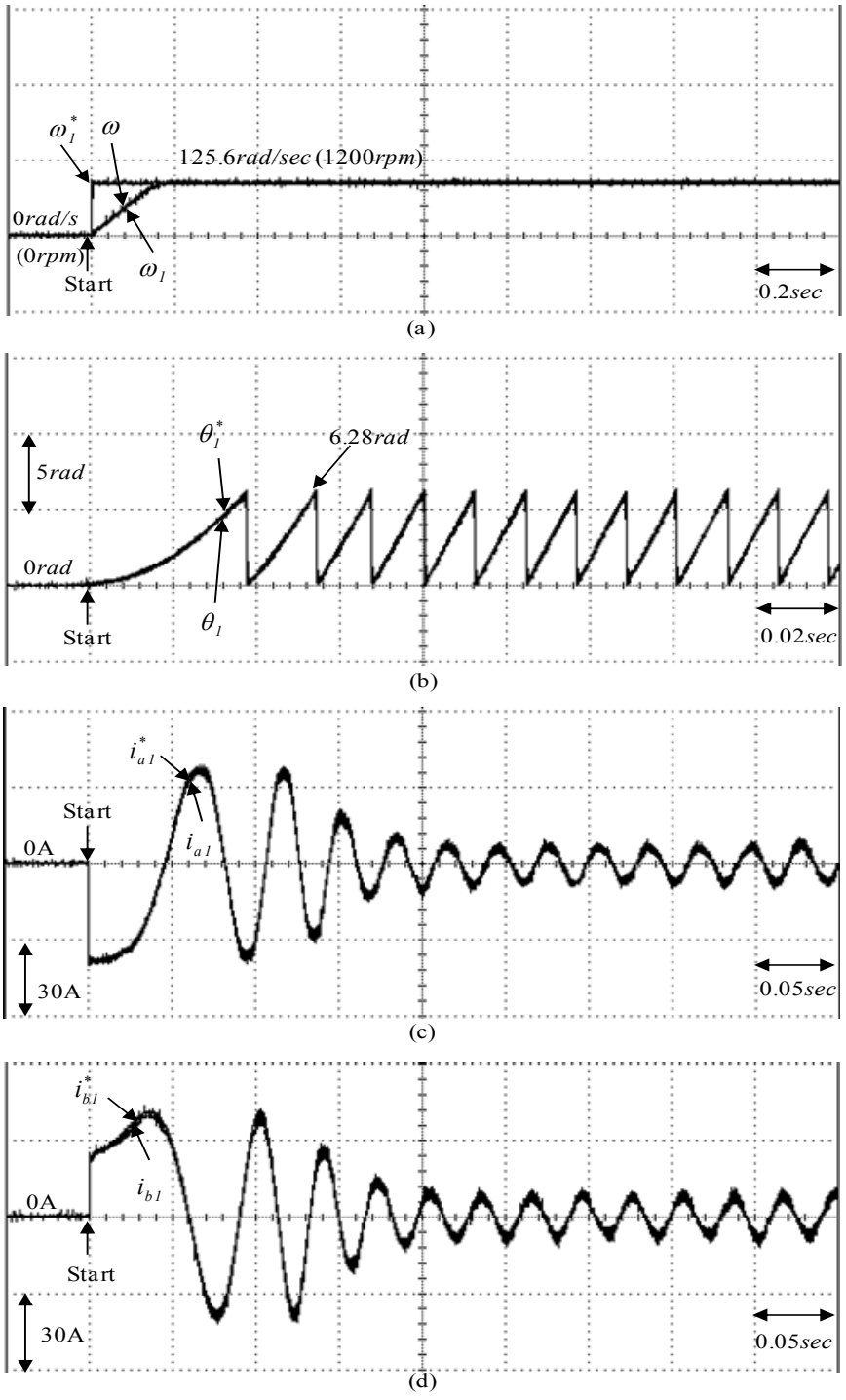

Fig. 6. Experimental results of the proposed novel hybrid modified Elman NN controlled for a PMSM drive electric scooter at 125.6 rad/sec (1200 rpm): (a) command rotor speed ω_1^*, desired rotor speed ω^* and measured rotor speed ω_1; (b) command rotor position θ^*, measured rotor position θ_1; (c) command current i_{a1}^* and measured current i_{a1} in phase $a1$; (d) command current i_{b1}^* and measured current i_{b1} in phase $b1$.

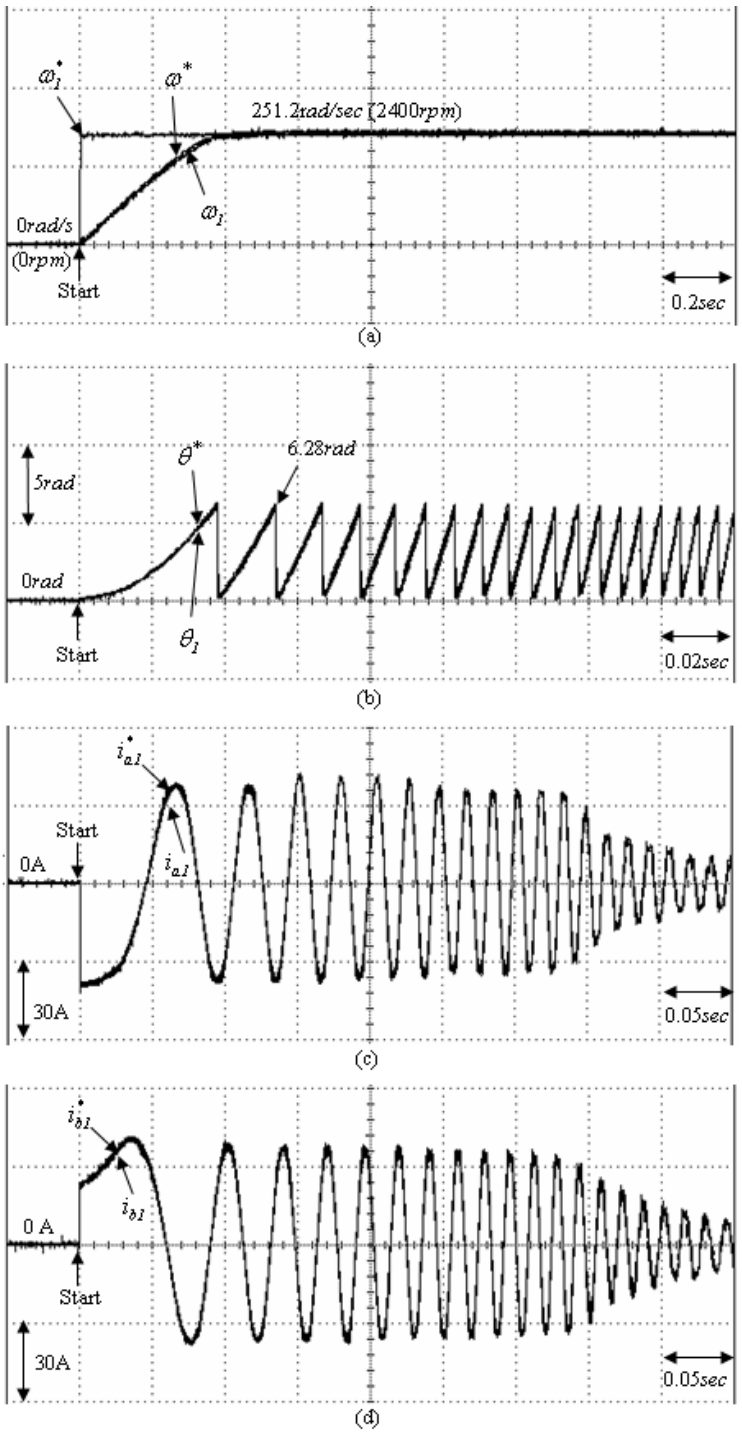

Fig. 7. Experimental results of the proposed novel hybrid modified Elman NN controlled for a PMSM drive electric scooter at 251.2 rad/sec (2400 rpm): (a) command rotor speed ω_1^*, desired rotor speed ω^* and measured rotor speed ω_1; (b) command rotor position θ^*, measured rotor position θ_1; (c) command current i_{a1}^* and measured current i_{a1} in phase $a1$; (d) command current i_{b1}^* and measured current i_{b1} in phase $b1$.

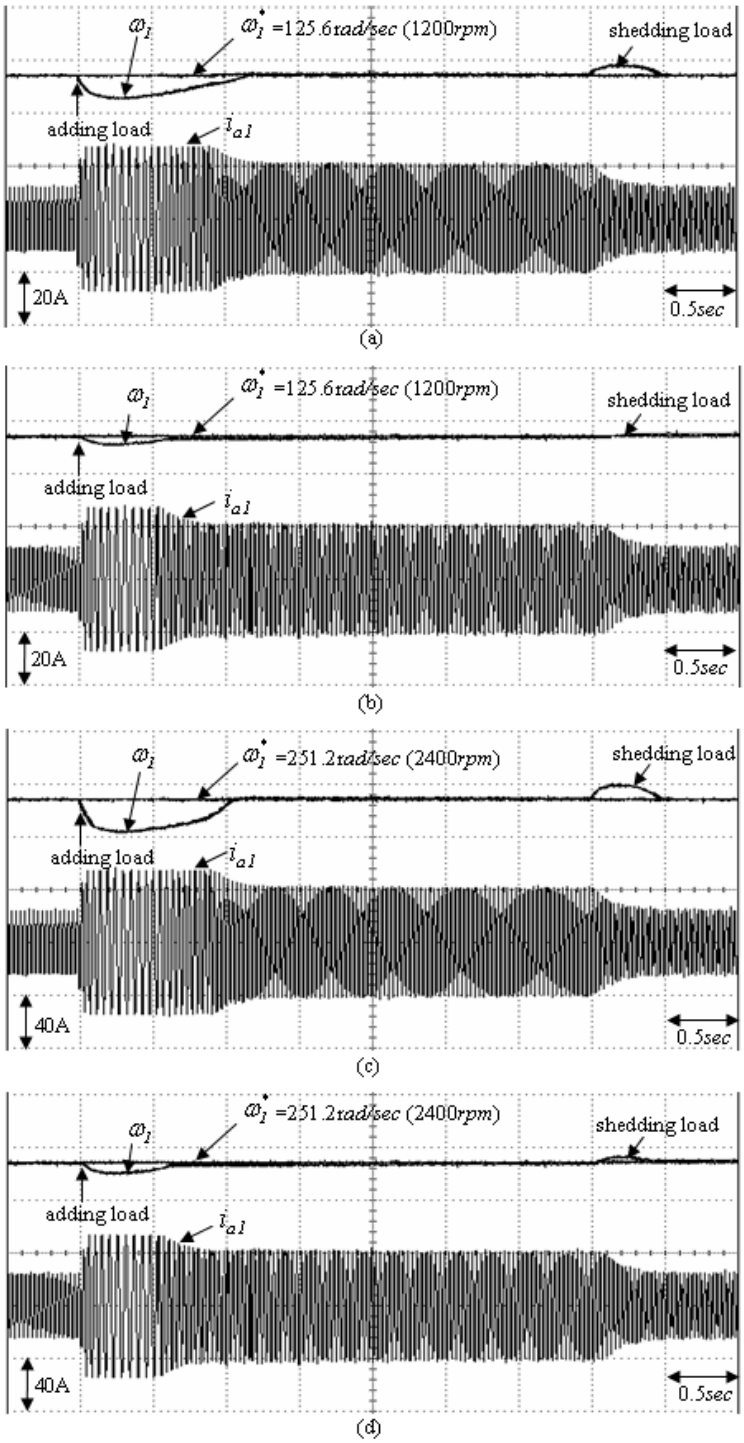

Fig. 8. Experimental results of the load torque disturbance with adding load and shedding load: (a) measured rotor speed ω_1 and measured current i_{a1} in phase $a1$ using the PI controller under $T_{L1} = 2$ Nm at the command rotor speed $\omega_1^* = 125.6$ rad/sec (1200 rpm); (b) measured rotor speed ω_1 and measured current i_{a1} in phase $a1$ using the proposed novel hybrid modified Elman NN control system under $T_{L1} = 2$ Nm at the command rotor speed $\omega_1^* = 125.6$ rad/sec (1200 rpm); (c) measured rotor speed ω_1 and measured current i_{a1}^* in phase $a1$ using the PI controller under $T_{L1} = 4$ Nm at the command rotor speed $\omega_1^* = 251.2$ rad/sec (2400 rpm); (d) measured rotor speed ω_1 and measured current i_{a1}^* in phase $a1$ using the proposed novel hybrid modified Elman NN control system under $T_{L1} = 4$ Nm at the command rotor speed $\omega_1^* = 251.2$ rad/sec (2400 rpm).

5. CONCLUSIONS

A PMSM drive system controlled by novel hybrid modified Elman NN control system has been successfully developed to drive electric scooter with the better control performance. First, the dynamic models of the PMSM drive system were derived according to electric scooter. Since the electric scooter is a nonlinear time varying system, sluggish speed tracking and weak load regulation are obtained for the PI controlled PMSM driven electric scooter due to the weak robustness of the linear controller from experimental results. Therefore, to ensure the better control performance, the PMSM controlled by novel hybrid modified Elman NN control system is developed to drive electric scooter. The novel hybrid modified Elman NN control system, which composed of the supervised control, the modified Elman NN and the compensated control, was proposed to reduce and smooth the control effort when the system states were inside the predetermined bound area. The novel hybrid modified Elman NN control system, which supervised control based on the uncertainty bounds of the controlled system, was designed to stabilize the system states around a predetermined bound area. Moreover, an on-line parameter training methodology is derived by using the Lyapunov stability theorem and the gradient descent method to increase the on-line learning capability of the modified Elman NN. From the experimental results, the control performance of the proposed novel hybrid modified Elman NN control system is more suitable than the PI controller for a PMSM driven electric scooter.

ACKNOWLEDGEMENT

The authors would like to acknowledge the financial support of the National Science Council in Taiwan, R.O.C., through its grant NSC 99-2221-E-239-040-MY3.

REFERENCES

1. Novotny, D.W. and Lipo, T.A., *Vector Control and Dynamics of AC Drives*, Oxford University Press, New York, 1996.
2. Leonhard, W., *Control of Electrical Drives*, Springer-Verlag, Berlin, 1996.
3. Lin, F.J., "Real-time IP position controller design with torque feedforward control for PM synchronous motor", *IEEE Transactions on Industrial Electronics*, Vol. 4, No. 3, pp. 398–407, 1997.
4. Elman, J.L., "Finding structure in time", *Cognitive Science*, Vol. 4, No. 2, pp. 179–211, 1990.
5. Arab, M.R., Suratgar, A.A., Martinez-Hernandez, V.M. and Rezaei Ashtiani, A., "Electroencephalogram signals processing for the diagnosis of petit mal and grand mal epilepsies using an artificial neural network", *Journal of Applied Research and Technology*, Vol. 8, No. 1, pp. 120–129, 2010.
6. Vargas-Martinez, A. and Garza-Castanon, L.E., "Combining artificial intelligence and advanced techniques in fault-tolerant control", *Journal of Applied Research and Technology*, Vol. 9, No. 2, pp. 202–226, 2011.
7. Jafari, A., "Artificial neural networks based approach for parametric optimization of CMOS operational amplifiers", *International Review of Electrical Engineering*, Vol. 4, No. 4, pp. 2032–2037, 2011.
8. Koker, R., "Design and performance of an intelligent predictive controller for a six-degree-of-freedom robot using the Elman network", *Information Sciences*, Vol. 176, No. 12, pp. 1781–1799, 2006.
9. Kalinli, A. and Sagiroglu, S., "Eleman network with embedded memory for system identification", *Journal Information Sciences Engineering*, Vol. 22, No. 6, pp. 1555–1568, November 2006.
10. Samek, D., "Elman neural networks in model predictive control", in *Proceedings of the 32rd European Conference on Modelling and Simulation*, pp. 577–584, 2009.
11. Chow, T.W.S. and Fang, Y., "A recurrent neural-network-based real-time learning control strategy applying to nonlinear systems with unknown dynamics", *IEEE Transactions on Industrial Electronics*, Vol. 145, No. 1, pp. 151–161, 1998.
12. Lu, C.H. and Tsai, C.C., "Adaptive predictive control with recurrent neural network for industrial processes: An application to temperature control of a variable-frequency oil-cooling machine", *IEEE Transactions on Industrial Electronics*, Vol. 55, No. 3, pp. 1366–1375, 2008.
13. Lin, C.H. and Lin, C.P, "Diagonal integral backstepping control for a PMLSM using adaptive RNNUO", *International Journal of Engineering and Technology Innovation*, Vol. 1, No. 1, pp. 53–64, 2011.

14. Liu, Q. and Wang, J., "Finite-time convergent recurrent neural network with a hard-limiting activation function for constrained optimization with piecewise-linear objective functions", *IEEE Transactions on Neural Networks*, Vol. 22, No. 4, pp. 601–613, 2011.
15. Cheng, L., Hou, Z.G., Lin, Y., Tan, M., Zhang, W.C. and Wu, F.X., "Recurrent neural network for non-smooth convex optimization problems with application to the identification of genetic regulatory networks", *IEEE Transactions on Neural Networks*, Vol. 22, No. 5, pp. 714–726, 2011.
16. Gao, X.Z., Gao, X.M. and Ovaska, S.J., "A modified eleman neural network model with application to dynamical systems identification", in *Proceedings of the IEEE International Conference on System, Man and Cybernetics*, pp. 1376–1381, 1996.
17. Yang, X.Y., Xu, D.P., Han, X.J. and Zhou, H.N., "Predictive functional control with modified Elman neural network for reheated steam temperature", in *Proceedings of International Conference on Machine Learning and Cybernetics*, pp. 4699–4703, 2005.
18. Lin, F.J., Teng, L.T. and Chu, H., "Modified elman neural network controller with improved particle swarm optimization for linear synchronous motor drive", *IET Electric Power Application*, Vol. 2, No. 3, pp. 210–214, 2008.
19. Li, J., Wu, H. and Pian, J., "The application of the equipment fault diagnosis based on modified Elman neural network", in *Proceedings of International Conference on Electronic and Mechanical Engineering and Information Technology*, pp. 4135–4137, 2011.
20. Lin, C.H. and Lin, C.P., "The hybrid rfnn control for a pmsm drive system using rotor flux estimator", in *Proceedings of International Conference on Power Electronics and Drive Systems*, pp. 1394–1399, 2009.
21. Lin, C.H., Chiang, P.H., Tseng, C.S., Lin, Y.L. and Lee, M.Y., "Hybrid recurrent fuzzy neural network control for permanent magnet synchronous motor applied in electric scooter", in *Proceedings of International Power Electronics Conference*, pp. 1371–1376, 2010.
22. Lin, F.J., Wai, R.J. and Hong, C.M., "Hybrid supervisory control using recurrent fuzzy neural network for tracking periodic inputs", *IEEE Transactions on Neural Networks*, Vol. 12, No. 1, pp. 68–90, 2001.
23. Slotine, J.J.E. and Li, W., *Applied Nonlinear Control*, Prentice-Hall, Englewood Cliffs, NJ, 1991.
24. Astrom, K.J. and Wittenmark, B., *Adaptive Control*, Addison-Wesley, New York, 1995.